Cancer Research

Cytotoxic Properties of a DEPTOR-mTOR Inhibitor in Multiple Myeloma Cells

Yijiang Shi[1], Tracy R. Daniels-Wells[2], Patrick Frost[1], Jihye Lee[3], Richard S. Finn[1], Carolyne Bardeleben[1], Manuel L. Penichet[2,4], Michael E. Jung[3], Joseph Gera[1], and Alan Lichtenstein[1]

Abstract

DEPTOR is a 48 kDa protein that binds to mTOR and inhibits this kinase in TORC1 and TORC2 complexes. Overexpression of DEPTOR specifically occurs in a model of multiple myeloma. Its silencing in multiple myeloma cells is sufficient to induce cytotoxicity, suggesting that DEPTOR is a potential therapeutic target. mTORC1 paralysis protects multiple myeloma cells against DEPTOR silencing, implicating mTORC1 in the critical role of DEPTOR in multiple myeloma cell viability. Building on this foundation, we interrogated a small-molecule library for compounds that prevent DEPTOR binding to mTOR in a yeast-two-hybrid assay. One compound was identified that also prevented DEPTOR–mTOR binding in human myeloma cells, with subsequent activation of mTORC1 and mTORC2. In a surface plasmon resonance (SPR) assay, the compound bound to recombinant DEPTOR but not to mTOR. The drug also prevented binding of recombinant DEPTOR to mTOR in the SPR assay. Remarkably, although activating TORC1 and TORC2, the compound induced apoptosis and cell-cycle arrest in multiple myeloma cell lines and prevented outgrowth of human multiple myeloma cells in immunodeficient mice. *In vitro* cytotoxicity against multiple myeloma cell lines was directly correlated with DEPTOR protein expression and was mediated, in part, by the activation of TORC1 and induction of p21 expression. Additional cytotoxicity was seen against primary multiple myeloma cells, whereas normal hematopoietic colony formation was unaffected. These results further support DEPTOR as a viable therapeutic target in multiple myeloma and suggest an effective strategy of preventing binding of DEPTOR to mTOR. *Cancer Res; 76(19); 5822–31. ©2016 AACR.*

Introduction

DEPTOR is an mTOR-binding protein that suppresses mTOR kinase activity (1–5). DEPTOR RNA expression is low in most malignancies (1), consistent with its role as an mTOR inhibitor. However, a remarkable upregulated expression of DEPTOR was singularly identified in the multiple myeloma model, especially in multiple myeloma tumors containing IgH gene translocations (1). Most importantly, DEPTOR silencing in overexpressing multiple myeloma cell lines resulted in growth arrest, suggesting it could be a therapeutic target (1). In a recent study (5), we identified a cascade where DEPTOR connected to an mTORC1/p21 survival pathway. It is counterintuitive that DEPTOR silencing with resulting mTOR activation should prevent multiple myeloma viability/proliferation, whereas growth factor (IL6/IGF)-induced proliferative responses are promoted by mTOR activation (6). One explanation for this dichotomy may be that acute mTORC1 activation due to DEPTOR silencing resulted in p21 upregulation, whereas during IL-6/IGF-induced mTOR activation, there is concurrent inhibition of p21 expression (7). DEPTOR may also promote multiple myeloma growth by repressing a negative feedback loop, resulting in activation of the PI3K/AKT survival pathway (1) or by restricting TORC1-mediated protein translation, which would protect against endoplasmic reticulum (ER) stress (8).

The anti-multiple myeloma effect of DEPTOR silencing was prevented by RAPTOR knockdown and paralyzed TORC1 activity (1, 5). This suggests that a DEPTOR/mTOR interaction within TORC1 complexes is key to the survival pathway. We, thus, interrogated a small-molecule library for compounds that prevented DEPTOR binding to mTOR in a yeast-two-hybrid (Y2H) screen. In this report, we describe the potential of a lead compound that prevented DEPTOR/mTOR binding in multiple myeloma cells with significant antitumor cytotoxicity, which is quite specific for multiple myeloma cells.

Materials and Methods

Cell lines, plasmids

All cell lines were obtained from ATCC. The cell lines were characterized by FISH analysis and proven to have MAF/Ig, MMSET/Ig, or D-cyclin/Ig translocations. All the cell lines were tested for mycoplasma within the last 6 months and were negative. The shRNAs targeting raptor and p21, the inducible

[1]Department of Hematology-Oncology, University of California at Los Angeles, Los Angeles, California. [2]Department of Surgery, University of California at Los Angeles, Los Angeles, California. [3]Department of Chemistry and Biochemistry, University of California at Los Angeles, Los Angeles, California. [4]Department of Microbiology, Immunology, and Molecular Genetics, University of California at Los Angeles, Los Angeles, California.

Note: Supplementary data for this article are available at Cancer Research Online (http://cancerres.aacrjournals.org/).

Corresponding Author: Alan Lichtenstein, University of California at Los Angeles, 11301 Wilshire Blvd, Bldg 304, Room E1-115, Los Angeles, CA, 90073. Phone: 310-268-3622; Fax: 310-268-4508; E-mail: alan.lichtenstein@med.va.gov

doi: 10.1158/0008-5472.CAN-16-1019

DEPTOR shRNA, and lentiviral transduction were previously described (5).

Drug screen

The Y2H yeast strain AH109 was cotransformed with two genes: the human DEPTOR gene fused to the GAL4 activation domain (AD) and the mTOR FAT domain fused to the GAL4 DNA-binding domain (DBD). Upon introduction of both vectors, DEPTOR/mTOR binding allows assembly of a transcription factor–inducing histidine synthesis and allowing growth on histidine-deficient media. Only when both DEPTOR-AD and mTOR-DBD were co-expressed were yeast capable of growing on histidine-deficient media. When cotransformed yeast are exposed to an inhibitor library, compounds that interrupt binding of mTOR to DEPTOR would prevent yeast growth on histidine-depleted media and allow their identification. In 3 experiments, the Z' values were between 0.8 and 0.85, values confirming high robustness of the screen.

Evaluation of protein expression and kinase activation

Coimmunoprecipitation between mTOR and DEPTOR was assayed as described (1). Assessment of 4E-BP1 phosphorylation by fluorescence-activated cell sorting (FACS) analysis was performed as described (9). A TORC2 *in vitro* kinase assay was performed as described (10).

Xenograft experiments

8226 cells (5×10^6/mouse) were injected subcutaneously and when tumor volume reached 200 mm^3, mice were randomized to receive intraperitoneal injections of drug or vehicle alone (control). Additional mice were injected with $CD45^+$ 8226 cells (10^7/mice) intravenously and treated with drug or vehicle in daily intraperitoneal injections. Fifteen days later, mice were sacrificed, bone marrow was obtained, and flow cytometry performed for $CD45^+$ tumor cells.

Primary cells and hematopoietic colony formation

Purified multiple myeloma cells were isolated as described (11). Hematopoietic colony formation was assessed as previously described (12) on marrow cells purchased from Stem Cell Technologies.

Surface plasmon resonance

Drug-binding studies were performed as previously described (13). Briefly, purified recombinant mTOR complex proteins were immobilized on a BIAcore CM5 sensor chip, and analyte solutions were prepared in a standard BIAcore buffer. Binding was measured by observing the change in the surface plasmon resonance (SPR) angle as 30 μL of analyte (in BIAcore buffer) flowed over the sample for 3 minutes at 10 μL/min. K_D values were calculated with BIAcore's BIAevaluation software, version 4.1.

Statistical analysis

DEPTOR expression in lines was determined by densitometry of immunoblots. Correlations between DEPTOR expression and IC_{50} were calculated by Pearson correlation. A one-tailed *t* test was used to assess significance of differences in IC_{50} between 1^o samples containing IgH translocations and samples without IgH translocations. For all other analyses, the Student *t* test was used to determine significance.

Results

Identification of an inhibitor

Initial efforts at confirming a yeast-two-hybrid (Y2H) interaction between mTOR and DEPTOR were unsuccessful when using full-length constructs. However, fusing the GAL4DBD to the mTOR FAT domain, the minimal DEPTOR-binding region (1), and cotransforming yeast with the full-length DEPTOR-GAL4AD, allowed for a robust interaction. The Y2H interaction results in histidine synthesis allowing growth on histidine-depleted plates (Supplementary Fig. S1A). Yeast were then replated and approximately 160,000 compounds from the NCI/DTP inhibitor library were individually pinned into plates. A halo of absent yeast growth indicated a compound that prevented binding of the transfected proteins and histidine synthesis. Absent growth on concurrently assayed plates in histidine-replete media (counter-screen) identified compounds that were nonspecifically toxic to yeast (e.g., anti-fungal drugs). These compounds were considered false-positives and were discarded. Four compounds (Supplementary Fig. S1B) were selectively inhibitory to growth of transfected yeast on histidine-depleted media. Two of these (called drug C and D in Supplementary Fig. S1) might be expected to show nonspecific toxicity because of the maleimide portion of the molecule and, indeed, they were toxic to hematopoietic colony formation and were not further studied. The remaining compounds (A and B) did not affect colony formation. Drug NSC126405 (called drug B in Supplementary Fig. S1) is slightly more cytotoxic to multiple myeloma cell lines (MMCL) than drug A and we, thus, have focused on this compound (Fig. 1A) in this report. The Y2H screen was designed to identify compounds that prevented DEPTOR/mTOR binding in yeast. The ability of NSC126405 to also prevent DEPTOR/mTOR binding in OPM-2 multiple myeloma cells is shown in Fig. 1B and C. After exposure for 6 hours, immunoprecipitated mTOR binds considerably less DEPTOR (Fig. 1B). In contrast, as a control, NSC126405 had no effect on the binding of mTOR to RICTOR in these immunoprecipitates. Similarly, after exposure to NSC126405, immunoprecipitated DEPTOR binds significantly less mTOR (Fig. 1C). The compound also prevented mTOR/DEPTOR binding in an additional MMCL, 8226 cells (Supplementary Fig. S2A).

Since DEPTOR is an mTOR inhibitor (1), a compound preventing mTOR/DEPTOR binding should result in TORC1 activation. We, thus, exposed 3 DEPTOR-expressing MMCLs to NSC126405 for 6 hours and tested TORC1 activity by immunoblot for p70 phosphorylated on T389. As shown in Fig. 1D, this resulted in an activation of TORC1 in all 3 MMCLs. NSC126405 enhanced TORC1 activity in 8226 cells rapidly by 2 hours of exposure (Fig. 1E). Exposure to NSC126405 also resulted in enhanced phosphorylation of 4E-BP1, another TORC1 substrate (Fig. 1F, immunoblot assay). In an additional assay for 4E-BP1 phosphorylation, we utilized flow cytometry (9) where MMCLs were stained for 4E-BP1 phosphorylation on T37/46. Supplementary Fig. S2B demonstrates a representative experiment, where control 8226 cells (DMSO) contain 3 populations of cells (A, B, and C) with distinct levels of 4E-BP1 phosphorylation. While exposure to pp242, an inhibitor of TORC1, resulted in loss of the phospho-4E-BP1 staining in

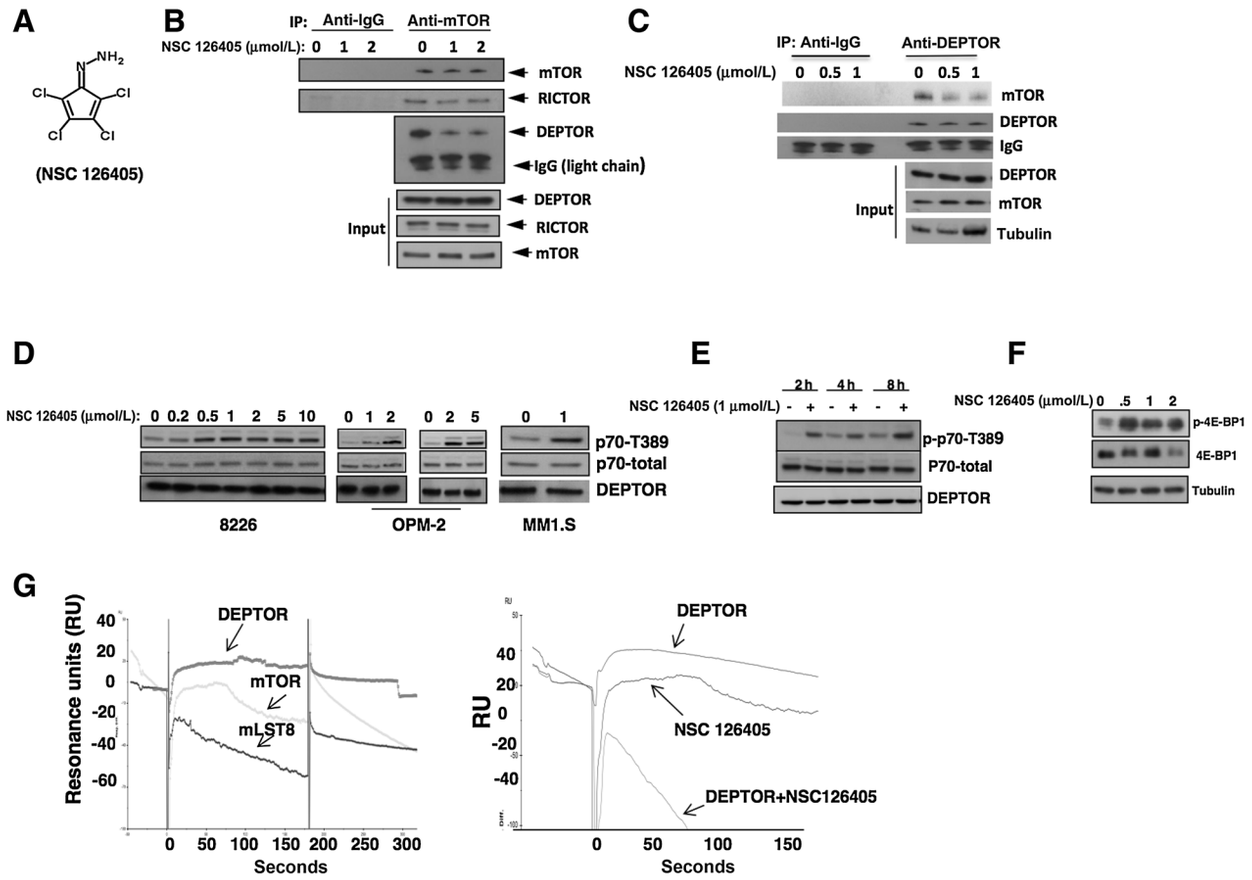

Figure 1.

Identification of an inhibitor preventing DEPTOR/mTOR binding. **A,** structure of NSC126405. **B** and **C,** OPM-2 cells treated with or without drug for 6 hours followed by immunoprecipitation of mTOR (**B**) or DEPTOR (**C**) and immunoblotting. **D,** MMCLs incubated with NSC126405 for 6 hours followed by immunoblot. **E,** 8226 cells treated with or without drug (1 μmol/L) for 2, 4, or 8 hours, followed by immunoblot assay. **F,** 8226 cells treated with or without drug, followed by immunoblot assay for 4E-BP1 phosphorylation. **G,** SPR assay: increasing concentrations of NSC126405 (100 μmol/L curve shown in figure) passed over immobilized DEPTOR, mTOR, or mLST8 to test binding partner of drug (left). Right, NSC126405 (100 μmol/L), recombinant DEPTOR (5 μg/mL), or combination of drug + DEPTOR passed over immobilized mTOR to assess binding.

populations B and C, exposure to NSC126405 significantly increased the population of cells with the greatest content of phosphorylated 4E-BP1 (from 44% to 74% in population C). Supplementary Fig. S2C summarizes the flow data from all 3 treatment groups. Since relatively few cells were required for this flow cytometric assay, it was ideal for studying molecular effects of NSC126405 in primary cells obtained from patients (see below).

To test whether NSC126405 prevents DEPTOR/mTOR binding by interacting with DEPTOR and/or mTOR, we utilized surface plasmon resonance (SPR). Recombinant DEPTOR, mTOR, or the mTOR-binding protein mLST8 were covalently cross-linked to the dextran matrix of a sensor chip and increasing concentrations of the compound were passed on these surfaces. Representative reference-subtracted overlaid sensorgrams are displayed in Fig. 1G (left). As shown, NSC126405 bound to immobilized DEPTOR rapidly and reached an equilibrium plateau within seconds. The K_D value was 3 μmol/L as derived from steady-state affinity determinations. In contrast, NSC126405 was incapable of binding to mTOR or mLST8. Although NSC126405 could not bind immobilized mTOR, recombinant DEPTOR successfully bound to immobilized mTOR (right). We then tested whether coinjected drug could prevent binding of DEPTOR to mTOR in the SPR assay. As shown (right), when NSC126405 is coinjected with DEPTOR, binding of the latter protein to cross-linked mTOR is prohibited. These results support the notion that the molecular target of drug B is DEPTOR with subsequent inhibition of DEPTOR/mTOR binding.

Cytotoxicity of NSC126405

Initial studies with 8226 cells demonstrated a concentration- and time-dependent inhibition of *in vitro* growth due to NSC126405 (Fig. 2A). A 3-day exposure was optimal for cytotoxicity. We then studied additional MMCLs and attempted to relate sensitivity to NSC126405 with level of DEPTOR expression. Since DEPTOR expression can be regulated posttranscriptionally (2–4), we assessed relative expression in MMCLs by immunoblot with quantification by densitometric analysis of DEPTOR/tubulin ratios. Comparison between cell lines was made on equally exposed immunoblots with consistent

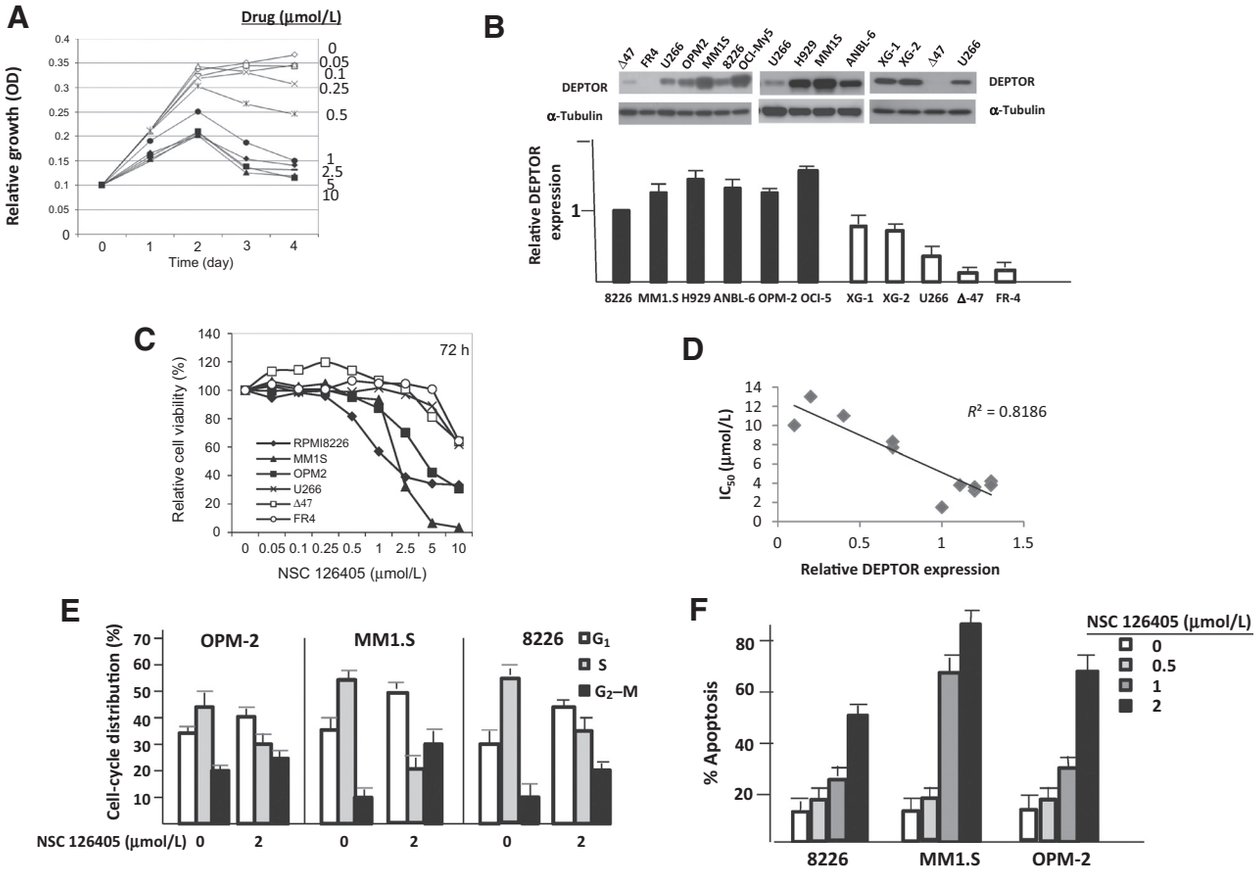

Figure 2.

Cytotoxicity of NSC126405. **A,** MTT assay of 8226 cells treated for 24 to 96 hours with NSC126405. **B,** DEPTOR protein expression in MMCLs (top) and relative DEPTOR/tubulin expression (mean ± SD, $n = 3$–7) assayed by immunoblot and densitometric analysis (bottom). Relative DEPTOR expression of 8226 cells arbitrarily designated "1." **C,** example of an MTT assay testing 6 MMCLs. **D,** correlation between NSC126405 sensitivity and relative DEPTOR expression. IC_{50} in μmol/L determined for all MMCLs exposed to drug for 72 hours and is presented as means of 3 to 6 individual experiments. Relative DEPTOR expression is taken from **B** and represents mean DEPTOR/tubulin expression, $n = 3$–7. **E,** cell-cycle distribution in MMCLs exposed with or without NSC126405 (2 μmol/L) for 48 hours. Data are mean ± SD, $n = 3$. NSC126405 caused a significant alteration ($P < 0.05$) in G_1, S, and G_2–M distribution. **F,** percentage of apoptosis in with or without cell lines exposed to drug for 72 hours. Data are mean ± SD, $n = 3$.

inclusion of the 8226 cell line in the blots and designating the DEPTOR/tubulin ratio of 8226 cells as `1'. In 15 immunoblot assays assessing DEPTOR/tubulin ratios in 8226 cells by densitometry, the SD was <5% of the mean, indicating that DEPTOR expression in 8226 cells assayed by immunoblot is very consistent between individual experiments. Examples of immunoblot assays are shown in Fig. 2B (top) with DEPTOR/tubulin ratios shown in the lower panel as mean ± SD, $n = 3$–7. Most of the MMCLs demonstrated high DEPTOR protein expression comparable to the 8226 line except for FR4 and Δ47 lines, whose expression was very low and the XG-1, XG-2, and U266 cell lines, which had intermediate expression. The high DEPTOR-expressing lines (black bars) either contain IgH-MAF translocations or IgH-MMSET translocations. The relatively high expression of DEPTOR in the MAF-translocated lines can be explained by the fact that DEPTOR is a transcriptional target of MAF (1). High DEPTOR expression in MMSET-translocated lines may be due to the fact that MMSET secondarily results in MAF expression (14).

As 72-hour exposure seemed optimal for cytotoxicity (Fig. 2A), we assayed all MMCLs in 72-hour MTT assays (example in Fig. 2C). 8226 cells were quite sensitive so we included them in each MTT assay as a positive control to ensure continued effectiveness of NSC126405 and accuracy of the assay. The mean IC_{50} for drug cytotoxicity against 8226 cells was 1.3 μmol/L ($n = 7$) and the SD was again <5% of the mean, indicating the consistency of the MTT assays and continued drug effectiveness. The MTT assays (example in Fig. 2C) show a concentration-dependent cytotoxicity of NSC126405. As shown, the DEPTOR-high expressing 8226, MM1.S, and OPM-2 lines appear significantly more sensitive than the lower expressing U266, Δ47, and FR4 multiple myeloma lines. We plotted the relative DEPTOR expression of the 11 MMCLs tested in Fig. 2B against their IC_{50} values (calculated from 3–7 MTT assays) and there is a significant inverse correlation as shown in Fig. 2D. The cytotoxicity of NSC126405 to MMCLs included cell-cycle arrest (Fig. 2E) and apoptosis (Fig. 2F). Cell-cycle arrest consisted of a combination of G_1–S and G_2–M arrest.

We also tested 6 hepatocellular carcinoma (HCC) cell lines as HCCs may overexpress DEPTOR to varying degrees (15). Although 3 HCC lines expressed DEPTOR in levels comparable to U266 and FR4 MMCLs (Supplementary Fig. S3A, bar graphs), they were unaffected by exposure to NSC126405 (Supplementary Fig. S3B). This suggests that the role of DEPTOR in survival/proliferation is specific to the multiple myeloma model. Further support for this notion is shown in Supplementary Fig. S3C and S3D where DEPTOR knockdown in HCC cells had no effect as compared with a cytotoxic effect in DEPTOR-silenced MMCLs.

Molecular effects of NSC126405

In MMCLs, DEPTOR knockdown stimulates TORC1/p70S6K and the subsequent phosphorylation of IRS-1 on serine 312 and IRS-1 degradation results in a negative feedback inhibition of the PI3K/AKT pathway (1, 5). To investigate effects of NSC126405 on this feedback loop, we first assayed AKT phosphorylation. Unexpectedly, in contrast to effects of DEPTOR knockdown, NSC126405 enhanced AKT phosphorylation in MMCLs (Fig. 3A). The accompanying PARP cleavage (arrow) demonstrates the early initiation of apoptosis. To more specifically address the negative feedback loop, we employed an 8226 cell line containing a doxycycline-inducible DEPTOR shRNA (5). When DEPTOR was silenced by doxycycline, IRS-1 S312 phosphorylation was induced as expected with degradation of total IRS-1 (Fig. 3B). In contrast, if these cells were exposed to NSC126405, using a concentration inducing comparable p70 phosphorylation, IRS-1 phosphorylation did not occur. In a second independent experiment (Fig. 3C), IRS-1 phosphorylation did not occur in drug-treated cells even when assayed at multiple time points, ruling out the possibility that the inducible MMCL exhibited different kinetics of the effect of NSC126405. Without negative feedback, NSC126405 should increase AKT phosphorylation due to its activation of TORC2. To test this possibility, we performed a TORC2 *in vitro* kinase assay (Fig. 3D). Initial experiments demonstrated specific immunoprecipitation of RICTOR and its accompanying mTOR (left). When 8226 cells are treated

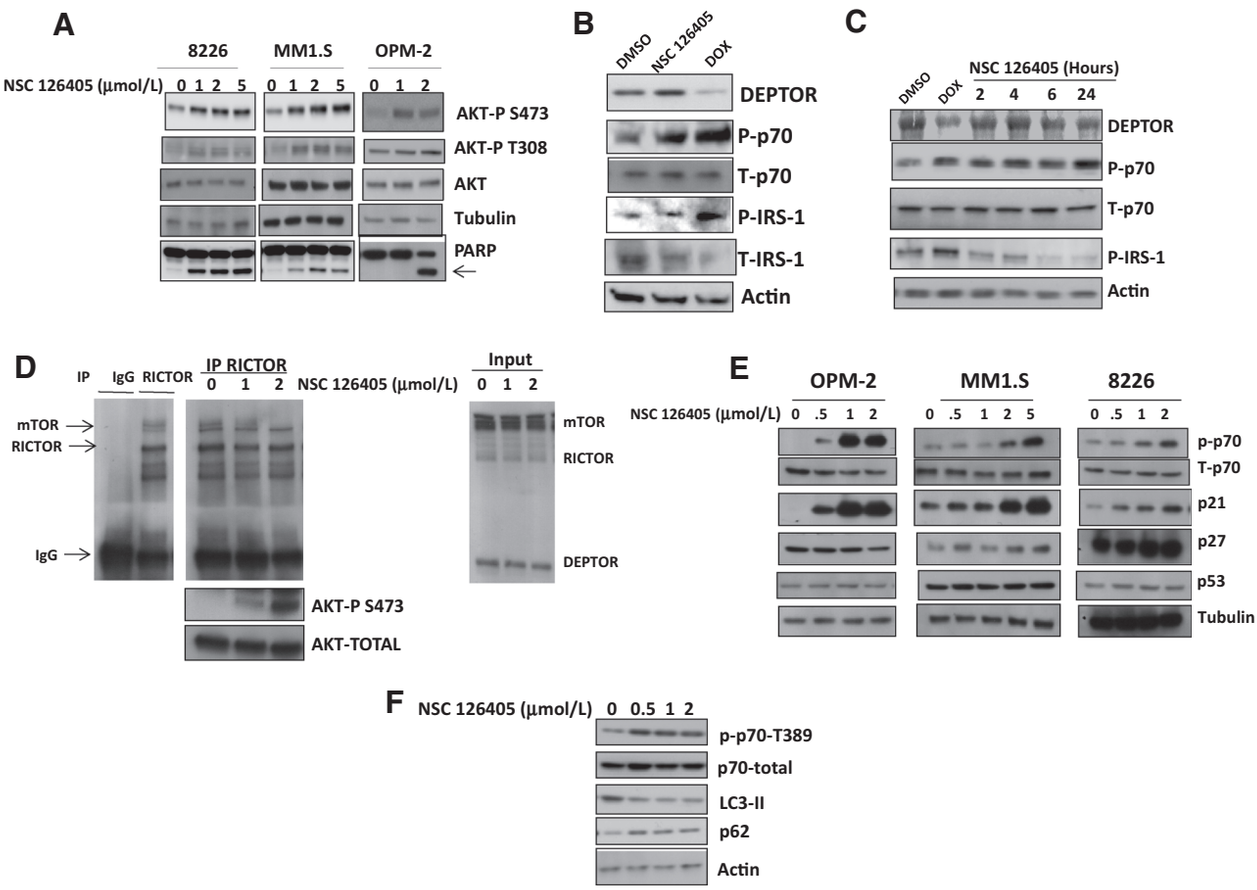

Figure 3.

Effect of NSC126405 on AKT. **A,** MMCLs exposed to NSC126405 for 6 hours, followed by immunoblot assay. **B,** doxycycline (dox)-inducible DEPTOR shRNA cells treated with DMSO (control), NSC126405 (2 μmol/L) for 6 hours, or doxycycline for 48 hours to induce DEPTOR shRNA. **C,** doxycycline-inducible DEPTOR shRNA cells treated with doxycycline for 48 hours or NSC126405 (2 μmol/L) for increasing intervals followed by immunoblot assay. **D,** TORC2 *in vitro* kinase assay. Left, 8226 lysate obtained and TORC2 complex immunoprecipitated by anti-RICTOR antibody (or IgG control), followed by immunoblot detection of mTOR and RICTOR. Middle, 8226 cells treated with 0, 1, or 2 μmol/L NSC126405 for 6 hours, after which TORC2 complex was immunoprecipitated by anti-RICTOR antibody and tested for its phosphorylation of AKT substrate on S473. Right, input. **E,** MMCLs treated with NSC126405 for 6 hours followed by immunoblot assay. **F,** 8226 cells treated with or without NSC126405 for 6 hours, followed by immunoblot assay.

with or without drug (1 or 2 μmol/L) for 6 hours, equal amounts of mTOR and RICTOR are immunoprecipitated (middle). When the immunoprecipitates are tested against AKT substrate (immunoblot below middle), it is apparent that NSC126405 has significantly enhanced TORC2-induced AKT phosphorylation.

We previously demonstrated (5) that DEPTOR knockdown induced p21 expression, which is independent of effects on p53 and which inhibited MMCL growth. Treatment of MMCLs with NSC126405 also induced p21 expression, which was concurrent with TORC1 activation (i.e., p70 phosphorylation, Fig. 3E). In contrast, there were no consistent effects on p53 or p27 expression.

Since mTORC1 activity is a key regulator of autophagy, we also assessed effects on autophagy. By increasing TORC1 activity, NSC126405 was expected to inhibit autophagy. Figure 3F confirms this expectation, as drug-treated cells show a decreased expression of LC3-II and an increased expression of p62, markers indicating decreased autophagic flux (16).

Role of TORC1, p21, and BCL proteins in drug B's cytotoxic effects

To test whether TORC1 activation induced by NSC126405 was relevant to cytotoxicity, we utilized 8226 cell lines with RAPTOR silenced by shRNA (5). Figure 4A demonstrates the efficiency of RAPTOR knockdown and the resulting inhibition of TORC1 activity. When RAPTOR-silenced cells are exposed to NSC126405 and compared with control [shScramble (SCR)], there is a significant decrease in resulting MTT cytotoxicity (Fig. 4B). There was also a significant decrease ($P < 0.05$) in induction of apoptosis assessed by flow cytometry at 72 hours (apoptosis values above bars in Fig. 4B). These data indicate that TORC1 activation is relevant to the anti–multiple myeloma effects of NSC126405.

To test the role of p21 induction, we utilized p21-knockdown 8226 cell lines transfected with 2 separate shRNAs as shown in Fig. 4C. Although p21 knockdown could not inhibit drug-induced apoptosis (data not shown), it significantly inhibited the G_1–S cell-cycle arrest (Fig. 4D). In control (scr-targeted shRNA) cells, G_1 distribution significantly increased at 1 and 2 μmol/L, whereas in both p21 knocked-down cell lines, G_1 distribution was not significantly altered. A corresponding decrease in S-phase distribution occurred in scr control cells exposed to 1 or 2 μmol/L, whereas little change was seen in p21 knocked-down cells. In contrast, the increase in G_2–M distribution found in control cells was also detected in p21-silenced cells. p21 knockdown, thus, specifically prevented the G_1–S arrest.

We also assessed levels of several proteins of the BCL family that have previously been shown (17, 18) to regulate apoptotic responses in multiple myeloma cells. After 4 hours of exposure to drug, there were no effects. However, at 18 hours, although there was no alteration in expression of BCL-2, MCL-1, BCL-XL, or PUMA, NSC126405 modestly induced upregulation of BIM (Supplementary Fig. S4A). When these experiments were repeated in RAPTOR-silenced cells, the drug-induced increase in BIM expression was abrogated (Supplementary Fig. S4B), suggesting that BIM upregulation was a result of TORC1 activation in DEPTOR-targeted cells.

Effect of NSC126405 *in vivo*

We tested toxicity of NSC126405 when injected intraperitoneally daily for 7 days. As shown in Fig. 5A, there was no significant weight loss during treatment or posttreatment. Red blood cell (RBC) counts performed after 7 days of treatment likewise showed no significant effect (Fig. 5B). Although 10 mg/kg of drug had no effect on WBC counts, a very modest but statistically significant decrease was seen at day +7 in mice injected with 20 mg/kg. Mice were also challenged subcutaneously with 8226 cells and, when tumors were palpable, they were randomized to receive either vehicle (control) or drug by daily injection for 11 days. As shown in Fig. 5C, both 10 and 20mg/kg of NSC126405 had an

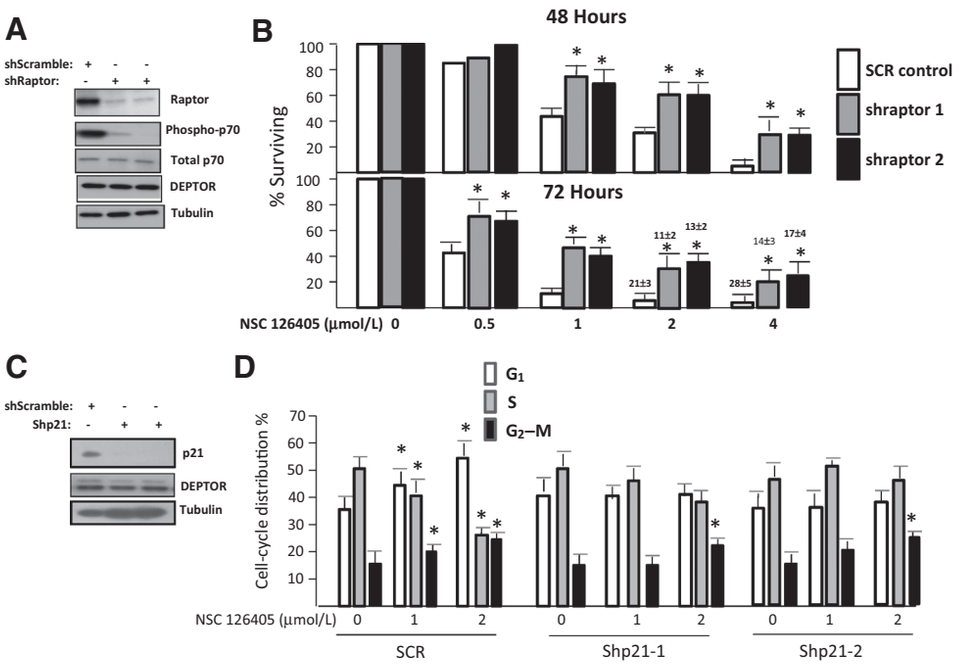

Figure 4.
Effect of RAPTOR and p21 shRNA. **A,** 8226 cells expressing shRNA targeting a scrambled sequence (control) or two separate sequences of RAPTOR, followed by immunoblot assay. **B,** MTT assay of control (SCR control) or RAPTOR-silenced 8226 multiple myeloma cells (shRaptor 1 and 2) challenged with NSC126405 for 48 or 72 hours. Data are mean ± SD, $n = 3$. *, significant difference ($P < 0.05$) from SCR control cells. Apoptosis (mean ± SD) is shown above 2 and 4 μmol/L bars in the 72-hour assay. **C,** 8226 cells expressing shRNA targeting scrambled sequence or two separate sequences of p21, followed by immunoblot assay. **D,** cell-cycle distribution of control (SCR) or p21-silenced multiple myeloma cells (Shp21-1 & Shp21-2) exposed to 0, 1, or 2 μmol/L NSC126405 for 48 hours. *, significant difference ($P < 0.05$) from control (0 μmol/L).

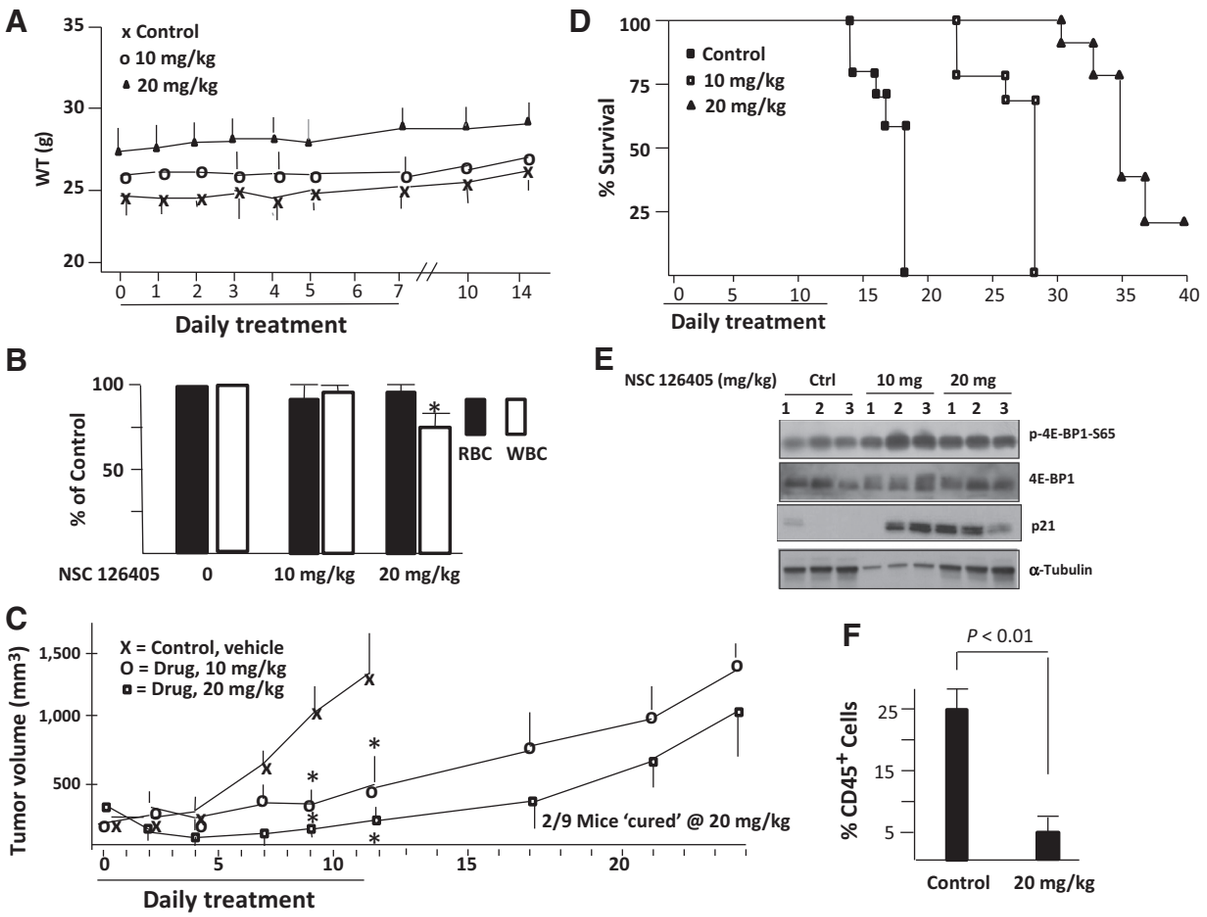

Figure 5.

Effect of NSC126405 in mice. **A,** weights (means, $n = 5$ mice/group) of mice treated with or without NSC126405 with daily intraperitoneal injections for 7 days. **B,** RBC and WBC counts in mice (5 mice/group) treated with daily intraperitoneal injections (7 days) of 0, 10, or 20 mg/kg NSC126405. Data are percentage of control. *, significant difference ($P < 0.05$) versus control. **C,** immunodeficienct mice (9 mice/group) challenged with 8226 cells subcutaneously, and when tumors became palpable, treatment initiated with daily intraperitoneal injections of vehicle control or NSC126405 for 11 days. Data represent tumor volume, mean ± SEM. *, significant differences ($P < 0.05$) from control. **D,** three tumors excised at random from treatment groups of **C** and probed for expression of phosphorylated 4E-BP1 and p21. **E,** mice challenged with CD45$^+$ 8226 multiple myeloma cells by intravenous injection ($n = 6$) and either treated with vehicle or NSC126405 (20 mg/kg) by intraperitoneal daily injection for 14 days. Mice were then sacrificed and CD45$^+$ multiple myeloma cells enumerated by flow cytometry. Our anti-human CD45 antibody did not stain any murine marrow cells in control marrow.

antitumor effect. In general, there was regrowth of tumors in these cohorts after the 11 days of treatment, although 2 of 9 mice treated with 20 mg/kg showed eradication of the tumor nodule without regrowth during an additional 1-month observation. The growth rate of individual tumors in these mice is shown in Supplementary Fig. S5. The increase in survival of drug-treated mice is shown in Fig. 5D. Tumors harvested from 3 mice per treatment group demonstrated enhanced 4E-BP1 phosphorylation (Fig. 5E) as expected from the putative activation of TORC1, as well as p21 upregulation.

Mice were also challenged with CD45$^+$ 8226 multiple myeloma cells injected intravenously to allow for dissemination within the skeleton. Mice were then treated with or without NSC126405 at 20 mg/kg/day intraperitoneally. After 14 days, bone marrow was harvested for human CD45 expression by FACS analysis. As shown (Fig. 5F), NSC126405 induced a reduction in CD45$^+$ 8226 multiple myeloma cells within the marrow.

Effect of NSC126405 on primary multiple myeloma cells

CD138$^+$ primary cells were isolated from newly diagnosed patients and exposed to NSC126405 for 48 hours, after which viable cells were enumerated by trypan blue staining in blinded fashion. A concentration-dependent anti–multiple myeloma effect was identified (Fig. 6A). Induction of apoptosis was also identified in a smaller number ($n = 4$) of primary specimens (Fig. 6B). In contrast, there were no toxic effects of NSC126405 when tested against normal peripheral blood lymphocytes (PBL; Supplementary Fig. S6). Since PBLs are nonproliferative, they may not be the most relevant control targets, so we also tested NSC126405 against marrow progenitors in colony-forming assays. As shown (Fig. 6C), there were no toxic effects when tested against colony formation. FISH data were obtained on all the multiple myeloma primary specimens, and the cytotoxic effect of NSC126405 was compared between cases with IgH translocations ($n = 7$) versus those without IgH translocations ($n = 10$; Fig. 6D). The FISH

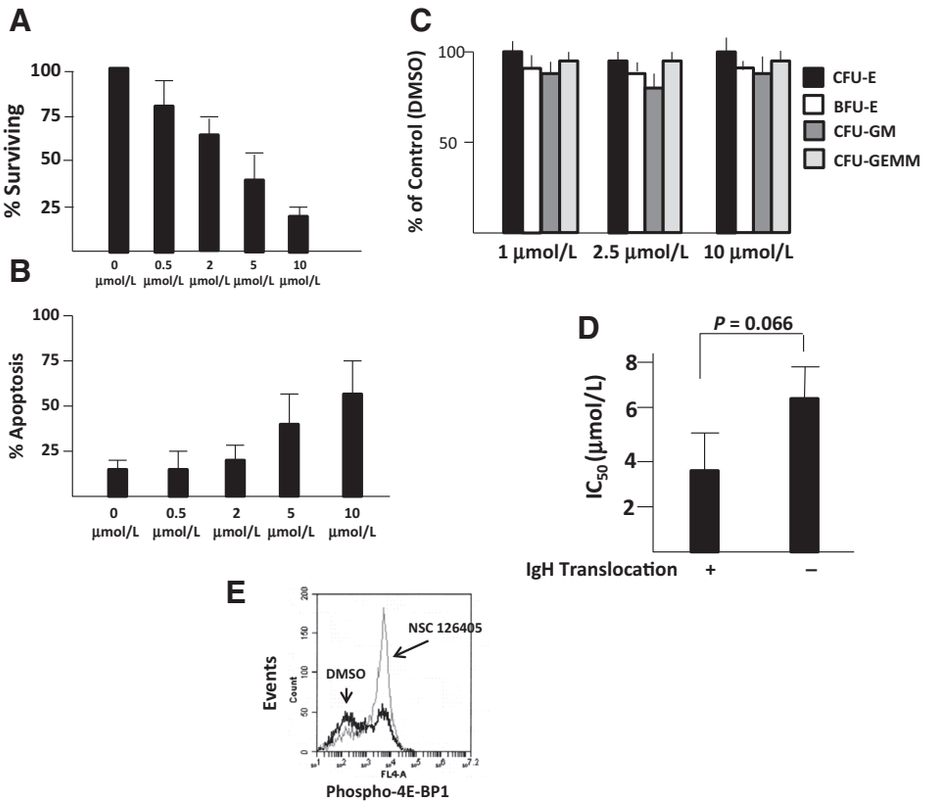

Figure 6.
Effect of NSC126405 on human cells. **A,** survival assay of CD138-isolated primary cells from patients ($n = 17$) exposed to NSC126405 for 48 hours. Data are percent surviving cells versus control (0 µmol/L), mean ± SD. **B,** flow cytometric analysis of apoptosis in four primary specimens incubated with NSC126405 for 48 hours. Data are mean ± SD. **C,** normal hematopoietic colony formation in cells exposed to NSC126405 for 14 days. Data represent percent of control (0 µmol/L), mean ± SD, $n = 4$. **D,** comparison of IC_{50} for NSC126405 between primary samples containing IgH translocations ($n = 7$) versus those without IgH translocations ($n = 10$). Data are means ± SEM. **E,** flow cytometric assay for 4E-BP1 phosphorylation in a primary multiple myeloma specimen.

abnormality in the latter specimens was hyperdiploidy. Although the calculated IC_{50} in specimens with IgH translocations was lower than those without IgH translocations, this difference was only present at the $P = 0.066$ level. Because of limitations in numbers of 1° cells harvested, we could not perform immunoblots to test for TORC1 activation following short-term drug exposure (4 hours). However, 3 specimens treated with or without NSC126405 (2 µmol/L) could be tested for 4E-BP1 phosphorylation using the flow cytometric assay described above in Supplementary Fig. S2B. There was an increase in cells with 4E-BP1 phosphorylation due to drug exposure (35% ± 7% in control vs. 59% ± 10%, in drug-treated cells, mean ± SD, $n = 3$ patient samples). An example of the flow analysis performed on one of the patients is shown in Fig. 6E.

Discussion

The current results further support the therapeutic potential of targeting DEPTOR in multiple myeloma and indicate that the association of DEPTOR with mTOR plays a critical role. Multiple DEPTOR-expressing MMCLs and primary cells were sensitive to NSC126405. The cytotoxic effect of NSC126405 was not promiscuous, as there were no significant adverse effects of the drug on normal PBLs, hematopoietic colony-forming cells, or HCC lines.

Recent progress in the development of inhibitors of protein–protein interactions has suggested the potential for such drugs (19–21). Our SPR data indicate that disruption of mTOR/DEPTOR binding is due to the initial interactions of NSC126405 with DEPTOR. The minimal mTOR-binding domain in DEPTOR is the PDZ domain (1). Although the structure of NSC126405 is not similar to other PDZ domain inhibitors (22, 23), it is possible that the drug interacts with the PDZ domain to prevent binding to mTOR. Alternatively, it may bind distally. Additional SPR experiments with truncated/mutated versions of DEPTOR are planned to better define the drug's binding area of the molecule.

Drug-induced cytotoxicity was restricted in a RAPTOR-silenced MMCL, indicating that activation of mTORC1 participates in the anti-myeloma cytotoxicity. However, it is not clear what molecular effects downstream of TORC1 mediate this activity. When we prevented p21 upregulation in multiple myeloma cells undergoing DEPTOR knockdown, we significantly protected against cell-cycle arrest as well as apoptosis (5). However, preventing p21 upregulation in drug-treated cells only protected against cell-cycle arrest. The ability of NSC126405 to upregulate proapoptotic BIM in a RAPTOR/TORC1-dependent fashion (Supplementary Fig. S4) may also participate in apoptosis. In addition, as autophagy is often cytoprotective in MMCLs (24, 25), the ability of NSC126405 to inhibit autophagy may play a role. In fact, the upregulated BIM expression may contribute to the inhibition of autophagy as previously shown in multiple myeloma cells (18).

A significant difference between DEPTOR silencing and NSC126405 exposure is the effect on AKT phosphorylation. DEPTOR knockdown results in stimulated TORC1 and TORC2 activity. However, stimulated TORC1 activity induces a negative feedback loop via TORC1-mediated phosphorylation of IRS-1, which inhibits PI3K signaling and results in depression of AKT phosphorylation, overcoming any activation of TORC2. In contrast, while NSC126405 similarly causes activation of TORC1 and TORC2, IRS-1 remains unaffected and the negative feedback is not

initiated. The activation of TORC2 in drug-treated cells is, thus, unopposed, resulting in stimulated AKT phosphorylation. It is not clear why a similar activation of mTORC1 activity induced by NSC126405 is unable to achieve IRS-1 S312 phosphorylation and feedback effects on PI3K/AKT. However, several previously reported studies (26, 27) also suggest lack of a simple direct correlation between DEPTOR-induced effects on mTORC1 and alteration of the negative feedback loop. Collectively, these results suggest that additional events (independent of TORC1) participate in regulation of IRS-1 phosphorylation. In our model, these events appear to be affected by DEPTOR knockdown but not by NSC126405.

It was remarkable that DEPTOR targeting, with subsequent activation of TORC1, TORC2, and AKT, results in MMCL cytotoxicity. This is especially so since previous work has demonstrated anti–multiple myeloma efficacy of dual TORC1/TORC2 inhibitors (28) as well as AKT inhibitors (29). However, several studies (1, 5) clearly demonstrate that the adverse effect of DEPTOR gene silencing in MMCLs is prevented by RAPTOR knockdown, thus implicating TORC1 activation. It is also clear from other studies (30, 31) that acute TORC1 activation, when occurring in a specific cell context, can result in tumor cell cytoreduction. As for TORC2 activation, in experiments not shown, RICTOR knockdown did not prevent drug cytotoxicity. Thus, TORC2 activation does not participate in the anti–multiple myeloma effect of NSC126405. However, because of its resulting activation of AKT, TORC2 may function to limit the efficacy of drug. Preliminary experiments with an AKT inhibitor, which enhanced NSC126405 efficacy (not shown), suggest this possibility.

Because previous work (1) indicated a strong correlation between DEPTOR RNA expression and multiple myeloma subgroups containing IgH translocations, we tested the hypothesis that sensitivity to our anti-DEPTOR drug would also correlate. Cytotoxicity to primary multiple myeloma cells, although somewhat related to FISH classification, did not reach statistical significance in 17 specimens studies. It is certainly possible that, with study of a larger cohort, there will be a statistically significant difference. However, a recent study (32) demonstrates an additional inducer of DEPTOR expression, CHE-1. As the presence of CHE-1 may not necessarily correlate with the IgH translocation subgroup, future studies to identify predictive markers of sensitivity to anti-DEPTOR therapy should investigate DEPTOR RNA or protein expression rather than simply FISH determined multiple myeloma classification.

Disclosure of Potential Conflicts of Interest

R.S. Finn is a consultant/advisory board member of Pfizer, Bayer, and Novartis. Dr. M.L. Penichet is a shareholder of Klyss Biotech, Inc. The Regents of the University of California are in discussions with Klyss to license Dr. Penichet's technology to this firm. No potential conflicts of interest were disclosed by the other authors.

Authors' Contributions

Conception and design: M.L. Penichet, J.F. Gera, A. Lichtenstein
Development of methodology: Y. Shi, R.S. Finn, M.L. Penichet, J.F. Gera
Acquisition of data (provided animals, acquired and managed patients, provided facilities, etc.): Y. Shi, T.R. Daniels-Wells, P. Frost, J. Lee, R.S. Finn, M.L. Penichet, M.E. Jung, J.F. Gera
Analysis and interpretation of data (e.g., statistical analysis, biostatistics, computational analysis): T.R. Daniels-Wells, P. Frost, R.S. Finn, C. Bardeleben, M.L. Penichet, J.F. Gera, A. Lichtenstein
Writing, review, and/or revision of the manuscript: T.R. Daniels-Wells, R.S. Finn, M.L. Penichet, J.F. Gera, A. Lichtenstein
Study supervision: M.L. Penichet

Grant Support

The study was supported by NIH grants KO1CA138559, 2RO1CA111448, 1RO1CA132778, RO1CA168700, RO1CA196266, P30A1028697, the UCLA AIDS Institute, funds of the VA and Multiple Myeloma Research Foundation. R. S. Finn received support from the Auerbach Family Gift for Emerging Therapies in Hepatocellular Carcinoma.

The costs of publication of this article were defrayed in part by the payment of page charges. This article must therefore be hereby marked *advertisement* in accordance with 18 U.S.C. Section 1734 solely to indicate this fact.

Received April 12, 2016; revised July 13, 2016; accepted July 15, 2016; published OnlineFirst August 16, 2016.

References

1. Peterson T, Laplante M, Thoreen C, Sancak Y, Kang S, Kuehl WM, et al. DEPTOR is an mTOR inhibitor frequently overexpressed in multiple myeloma cells and required for their survival. Cell 2009;137:1–14.
2. Duan S, Skaar J, Kuchay S, Toschi A, Kanarek N, Ben-Neriah Y, et al. mTOR generates an auto-amplification loop by triggering the beta TrCP- and CK1alpha-dependent degradation of DEPTOR. Mol Cell 2011;44:317–24
3. Gao D, Inuzuka H, Tan M, Fukushima H, Locasale JW, Liu P, et al. mTOR drives its own activation via $SCF^{\beta TrCP}$-dependent degradation of the mTOR inhibitor DEPTOR. Mol Cell 2011;44:290–303.
4. Luo Z, Yu G, Lee H, Li L, Wang L, Yang D, et al. The Nedd8-activating enzyme inhibitor MLN4924 induces autophagy and apoptosis to suppress liver cancer cell growth. Cancer Res 2012;72:3360–71.
5. Yang Y, Bardeleben C, Frost P, Hoang B, Shi Y, Finn R, et al. DEPTOR is linked to a TORC1-p21 survival proliferation pathway in multiple myeloma cells. Genes Cancer 2014;5:407–19
6. Shi Y, Hsu JH, Hu L, Gera J, Lichtenstein A. Signal pathways involved in activation of p70S6K and phosphorylation of 4E-BP1 following exposure of myeloma tumor cells to IL-6. J Biol Chem 2002277:15712–20.
7. Urashima M, Teoh G, Chauhan D, Hoshi Y, Ogata A, Treon SP, et al. IL-6 overcomes p21 upregulation and G1 growth arrest induced by dexamethasone and interferon-gamma in myeloma cells. Blood 199790:279–89.
8. Obeng EA, Carlson LM, Gutman DM, Harrington WJ, Lee K, Boise L. Proteasome inhibitors induce a terminal unfolded protein response in multiple myeloma cells. Blood 2006;107:4907–16.
9. Rizziere D, Feldman E, DiPersio J. A phase 2 clinical trial of deforolimus, a novel mTOR inhibitor, in patients with relapsed or refractory hematologic malignancies. Clin Cancer Res 2008;14:2756–62.
10. Huang J.An *in vitro* assay for the kinase activity of mTOR complex 2. Methods Mol Biol 2012;821:75–86.
11. Yoo EM, Trinh K, Tran D. Anti-CD138-targeted interferon is a potent therapeutic against multiple myeloma. J Interferon Cytokine Res 2015;35: 281–91.
12. Shi Y, Reiman T, Li W, Maxwell CA, Sen S, Pilarski L, et al. Targeting aurora kinases as therapy in multiple myeloma. Blood 2007;109:3915–21.
13. Chu H, Pazgier M, Jung G, Nuccio S-P, Castillo P, de Jong M, et al. Human alpha-defensin promotes mucosal innate immunity through self-assembled peptide nanonets. Science 2012;337: 477–81.
14. Annunziata CM, Hernandez L, Davis RE, Zingone A, Lamy L, Lam LT, et al. A mechanistic rationale for MEK inhibitor therapy in myeloma based on blockade of MAF oncogene expression. Blood 2011;117: 2396–404.

15. Yen C, Lu Y, Li C, Lee C-M, Chen C-Y, Cheng M-Y, et al. Functional characterization of glycine N-methyltransferase and its interactive protein DEPDC6/DEPTOR in hepatocellular carcinoma. Mol Med 2012; 18:286–96.
16. Klionsky DJ, Abeliovich H, Agostinis P. Guidelines for the use and interpretation of assays for monitoring autophagy in higher eukaryocytes. Autophagy 2008;4:151–75.
17. Morales A, Kurtoglu M, Matulis S, Liu J, Siefker D, Gutman D, et al. Distribution of BIM determines MCL-1 dependence or codependence with BCL-XL/BCL-2 in MCL-1-expressing myeloma cells. Blood 2011;118: 1329–39.
18. Chen S, Zhang Y, Zhou L, Leng Y, Lin H, Kmieciak M, et al. A BIM-targeting strategy overcomes adaptive bortezomib resistance in myeloma through a novel link between autophagy and apoptosis. Blood 2014;124:2687697.
19. Wells JA, McClendon CL. Reaching for high-hanging fruit in drug discovery at protein-protein interfaces. Nature 2007;450:1001–9.
20. Jin L, Wang W, Fang G. Targeting protein-protein interaction by small molecules. Annu Rev Pharmacol Toxicol 2014;54:435–56
21. Sheng C, Dong G, Miao Z, Zhang W, Wang W. State-of-the-art strategies for targeting protein-protein interactions by small-molecule inhibitors. Chem Soc Rev 2015;44:8238–59.
22. Daw M, Chittajallu R, Bortolotto Z, Dev K, Duprat F, Henley J, et al. PDZ proteins interacting with C-terminal GluR2/3 are involved in a PKC-dependent regulation of AMPA receptors at hippocampal synapses. Neuron 2000;28:873–86
23. Fujii N, You L, Xu Z, Uematsu K, Shan J, He B, et al. An antagonist of disheveled protein-protein interaction suppresses beta-catenin-dependent tumor cell growth. Cancer Res 2007;67:573–9.
24. Riz I, Hawley TS, Hawley RG. KLF4-SQSTM1/p62-associated pro-survival autophagy contributes to carfilzamib resistance in multiple myeloma models. Oncotarget 2015;6:17814–831
25. Malek MA, Jagannathan S, Malek E. Molecular chaperone GRP78 enhances aggresome delivery to autophagosomes to promote drug resistance in multiple myeloma. Oncotarget 2015;6:3098–110.
26. Chen R, Yang Q, Lee J-D. BMK1 kinase suppresses epithelial-mesenchymal transition through the AKT/GSK signaling pathway. Cancer Res 2012;72: 1579–87.
27. Liu M, Wilk S, Wang A, Zhou L, Wang R-H, Ogawa W, et al. Resveratrol inhibits mTOR signaling by promoting the interaction between mTOR and DEPTOR. J Biol Chem 2010;285:36387–94.
28. Cirstea D, Santo L, Hideshima T, Eda H, Mishima Y, Nemani N, et al. Delineating the mTOR kinase pathway using a dual TORC1/2 inhibitor, AZD8055, in multiple myeloma. Mol Cancer Ther 2014;13:2489–500.
29. Mimura N, Hideshima T, Shimomura T, Suzuki R, Ohguchi H, Rizq O, et al. Selective and potent AKT inhibition triggers anti-myeloma activities and enhances fatal ER stress induced by proteasome inhibition. Cancer Res 2014;74:4458–69.
30. Kato H, Nakajima S, Saito Y, Takahashi S, Katoh R, Kitamura M. mTORC1 serves ER stress-triggered apoptosis via selective activation of the IRE1-JNK pathway. Cell Death Diff 2012;19:310–20.
31. Astle MV, Hannan KM, Ng PY, Lee RS, George AJ, Hsu AK, et al. AKT induces senescence in human cells via mTORC1 and p53 in the absence of DNA damage: implications for targeting mTOR during malignancy. Oncogene 2012;31:1949–62.
32. Desantis A, Bruno T, Catena V, De Nicola F, Goeman F, Iezzi S, et al. Che-1-induced inhibition of mTOR pathway enables stress-induced autophagy. EMBO J 2015;34:1214–30.